AIP | Journal of Applied Physics

Vanishing critical thickness in asymmetric ferroelectric tunnel junctions: First principle simulations

Meng-Qiu Cai, Yue Zheng, Pui-Wai Ma, and C. H. Woo

Citation: J. Appl. Phys. **109**, 024103 (2011); doi: 10.1063/1.3532000
View online: http://dx.doi.org/10.1063/1.3532000
View Table of Contents: http://jap.aip.org/resource/1/JAPIAU/v109/i2
Published by the American Institute of Physics.

Vanishing critical thickness in asymmetric ferroelectric tunnel junctions: First principle simulations

Meng-Qiu Cai, Yue Zheng,[a] Pui-Wai Ma, and C. H. Woo[b]
Department of Electronic and Information Engineering, The Hong Kong Polytechnic University, Hong Kong Special Administrative Region, China

(Received 4 September 2010; accepted 26 November 2010; published online 19 January 2011)

The stability of the remnant polarization in the ferroelectric barrier layer is a prerequisite to applications involving ferroelectric tunnel junctions (FTJs) or capacitors. One of the most important issues in the pursuit of further developments in this area is to overcome the limitations due to the critical thickness, below which the ferroelectric polarization disappears. In this paper we report first-principle density-functional calculations of the charge distribution and polarization in an asymmetric FTJ (A-FTJ), i.e., one with dissimilar electrodes. We found that a significant and stable polarization can be retained down to thicknesses as small as 0.8 nm (two unit-cells) in a $BaTiO_3$ thin film between Pt and $SrRuO_3$ electrodes, quite unlike the case of symmetric FTJs. We trace this surprising result to the large electric field produced by the charge transfer between the electrodes caused by their different electronic environments, which acts against the depolarization field and enhances the ferroelectricity, leading to the reduction, or even the complete elimination of the depolarization field, leading to the vanishing of the critical thickness. We speculate that this is a general result for A-FTJs, which could be of importance to applications of ferroelectric thin films and tunneling junctions or capacitors where the presence of the critical thickness is a limiting factor. © *2011 American Institute of Physics*. [doi:10.1063/1.3532000]

I. INTRODUCTION

Ferroelectric tunnel junctions (FTJs) or capacitors using ferroelectric barriers in nanoscale show many interesting electronic transport properties,[1–7] such as giant electroresistance,[3,5,6] giant piezoresistance,[7] nondestructive read out,[1] etc. Many of them present attractive prospects of applications in the functional design of nanotransducers, ultrahigh-density nonvolatile random-access memories, ferroelectric nanodiodes, and other nanoferroelectric devices. Generally speaking, the most important and useful characteristic of a FTJ is the orders of magnitude change in the tunneling conductance it may display in response to moderate changes in the polarization in the tunnel barrier. Naturally, the stability of the ferroelectric state in the tunnel barrier is crucial to all these wonderful possibilities.

It is well known that the polarization in a ferroelectric thin film (FTF) can only be retained above some critical thickness of about 1–10 nm, due to surface and interface effects.[8–18] Obviously, a large critical thickness necessarily puts some rather stringent limitations on the practicality of many novel designs in the nanoregime involving ferroelectric materials. A good understanding of the factors governing the critical thickness might thus help a long way toward the full utilization of FTJs in nanodevices.

Early studies of the size effects on critical properties of the FTF gave the impression that the critical size of the FTF was a few tens of nanometers.[19] More recent experiments and theoretical calculations found that the critical size is much smaller. Thus, Tybell *et al.*[8] demonstrated the presence of a stable polarization in a 4-nm-thick epitaxial film of the perovskite ferroelectric $PbZr_{0.2}Ti_{0.8}O_3$ at room temperature by combining electric-force microscopy and piezoelectric scanning-probe microscopy. Fong *et al.* adopted x-ray scattering and observed ferroelectric properties of epitaxial $PbTiO_3$ films down to 1.2 nm, showing 180° stripe domains on $SrTiO_3$ insulator substrate[9] but monodomain structure on conducting $SrRuO_3$ (SRO) electrode with surface ionic adsorbates.[10] Using variable-temperature ultraviolet Raman spectroscopy, Tenne *et al.*[11] found that the critical size of strained $BaTiO_3$ (BTO) films grown on the $SrTiO_3$ substrate is about 1.6 nm. Kim *et al.* obtained a critical thickness of about 5 nm for the fully strained $SrRuO_3/BaTiO_3/SrRuO_3$ heterostructure on $SrTiO_3$ substrates by pulsed-laser deposition with *in situ* reflection high-energy electron diffraction. Moreover, it was found that ferroelectricity can exist in ferroelectric polymers thin films with monolayer thickness.[12,13] Results based on first-principle simulation[14,20–25] and first-principle effective Hamiltonian method[28] also predicted that the critical thickness in the perovskite films could be down to just a few lattice parameters. For example, the first-principles calculations of Junquera and Ghosez[14] predicted a critical size of about 2.4 nm for FTFs with symmetrical electrodes such as $SrRuO_3/BaTiO_3/SrRuO_3$. In the thermodynamic approach, Wang and Woo[15] related the FTF thickness to the Curie temperature through the dynamic instability of the free-energy functional, and derived explicit expressions for the critical thickness. Zheng and Woo[16] adopted a similar approach for the symmetric FTJ (S-FTJ). Both works estimated that the critical thicknesses for BTO was between 1 and 2 nm, consistent with the other works in this area.[26,27]

[a]Electronic mail: zhengy35@mail.sysu.edu.cn.
[b]Electronic mail: chung.woo@polyu.edu.hk.

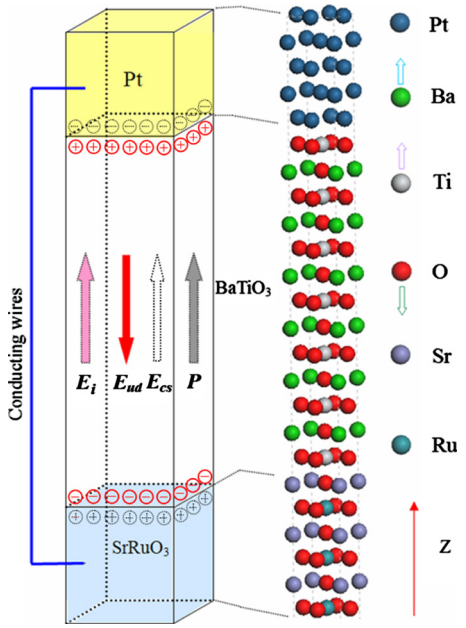

FIG. 1. (Color online) Schematic configuration of the system adopted in the present calculations for a typical A-FTJs. The arrows denote the directions of the polarization P, unscreened depolarization field E_{ud}, charge screening electric field E_{cs} and built-in electric field E_i.

Absent the surface relaxation and the constraint of the thick substrate or electrodes, the critical size of ultrathin FTFs under short circuit boundary conditions can be attributed predominantly to the depolarization field arising from the incomplete screening in the electrodes and interfaces, which has a strength as high as 10^8 V/m.[14,16,26] In this regard, the destabilizing effect due to the interface in ultrathin-film devices has been formulated in terms of a reduced interface capacitance, or equivalently an effective dead layer in contact with the electrodes.[25–30]

In S-FTJs, i.e., one with similar electrodes, typical critical thicknesses have been established at around 2 nm.[14,16] It is natural to ask whether useful changes could be brought about by replacing one of the electrodes with a different conductor, resulting in an asymmetric FTJ (or A-FTJ), i.e., one with dissimilar electrodes. This is a question that can only be reliably answered via first-principle calculations. In this regard, we will consider the case of an ultrathin barrier of $BaTiO_3$ sandwiched between dissimilar electrodes made from metallic platinum Pt and strontium ruthenate $SrRuO_3$, epitaxially grown on a thick $SrTiO_3$ substrate (Fig. 1). We note that both Pt and $SrRuO_3$ are perfect electrode materials for ferroelectric nanodevices.

II. THEORETICAL APPROACH

Total energy calculations are performed within the density-functional theory using ultrasoft Vanderbilt pseudopotentials method implemented in the VIENNA *AB INITIO SIMULATION PACKAGE*.[31] The exchange-correlation potential is treated in the local density approximation using the Ceperly–Alder scheme.[32] We note that the commonly used general gradient approximation (GGA) functional might not be entirely satisfactory for the present purpose.[33] An energy cutoff of 500 eV is used for a plane wave basis, with a $6\times6\times1$ Monkhorst–Pack grid for k-point sampling. Following Ref. 14, we use the theoretical lattice constant of cubic $SrTiO_3$ (3.8668 Å) as the in-plane lattice constant of the superlattice of the whole structure. We use this procedure to simulate the misfit strains on Pt, $SrRuO_3$, and $BaTiO_3$ due to the substrate. This compressive misfit strain due to the substrate helps maintain the in-plane ferroelectric stability of the $BaTiO_3$ thin film. Relaxation of bulk Pt, $SrRuO_3$, and $BaTiO_3$ lattices are performed under this constraint, and the resulting tetragonal unit cells are used as the building blocks for the supercell. We note that the relaxation increases the polarization of the $BaTiO_3$ from 0.187 to 0.235 C/m^{-2}, calculated using the Berry phase method.[34]

We consider a supercell geometry, in which the $SrRuO_3$ (001) and Pt (001) electrode layers are separated by a ferroelectric $BaTiO_3$ (001) layer (Fig. 1). Due to the volatility of Ru, Pt/TiO_2 and SrO/TiO_2 interfaces with the $BaTiO_3$ film are expected, and are thus assumed in our calculations. The basic unit, to be periodically repeated in the x- and y-directions, is illustrated in Fig. 1 and corresponds to the generic formula $[Pt_{10}/TiO_2-(BaO-TiO_2)_n-(SrO-RuO_2)_3]$, n ranging from 2 to 10. In general, short-circuit boundary conditions are employed and implemented via the periodic boundary conditions, which are valid in the ferroelectric/metal capacitor structure when the thicknesses of the electrodes reach about five to seven layers.[35] In our configuration, the thicknesses of the $SrRuO_3$ and Pt electrodes are 3.5 and 2.5 unit cells, respectively.

Ferroelectric polarization is generally the result of the relative displacement of the charge centers of the cations and anions. In the present case, it can be separated into contributions from the Ti–O and Ba–O atomic layers.[36,37] The discontinuity at the ferroelectric/electrode interface produces depolarization charges that give rise to the well-known depolarization field. Charge redistributions in the electrodes due to the presence of the depolarization charges screen the depolarization field and maintain the stability of the ferroelectric state.[14] An all-atomic relaxation that includes the atoms of both electrodes must therefore be performed. In this way, starting from the atomic configuration of paraelectric $BaTiO_3$, calculations are performed for various thicknesses of $BaTiO_3$, from $n=2$ to 10. We note that atomic relaxations are only needed along the z-direction, following the displacement pattern of the bulk tetragonal soft mode (as shown in Fig. 1), because the constraint of the $SrTiO_3$ substrate is only in the xy-plane. The relaxation is continued until the maximum Hellman–Feynman force acting on each atom is less than 10 meV/Å. Only single domain configurations are considered and a compressive stress is applied laterally, consistent with experiments.

III. RESULTS AND DISCUSSION

A. The relative Ti–O and Ba–O displacements

In Fig. 2 we show the relative anion-cation displacements (RACDs) in the z-direction along the bulk tetragonal soft mode in (a) the Ti–O layer (to be referred to as the Ti–O displacement in the following) and (b) the Ba–O layer (to be referred to as the Ba–O displacement in the following). In

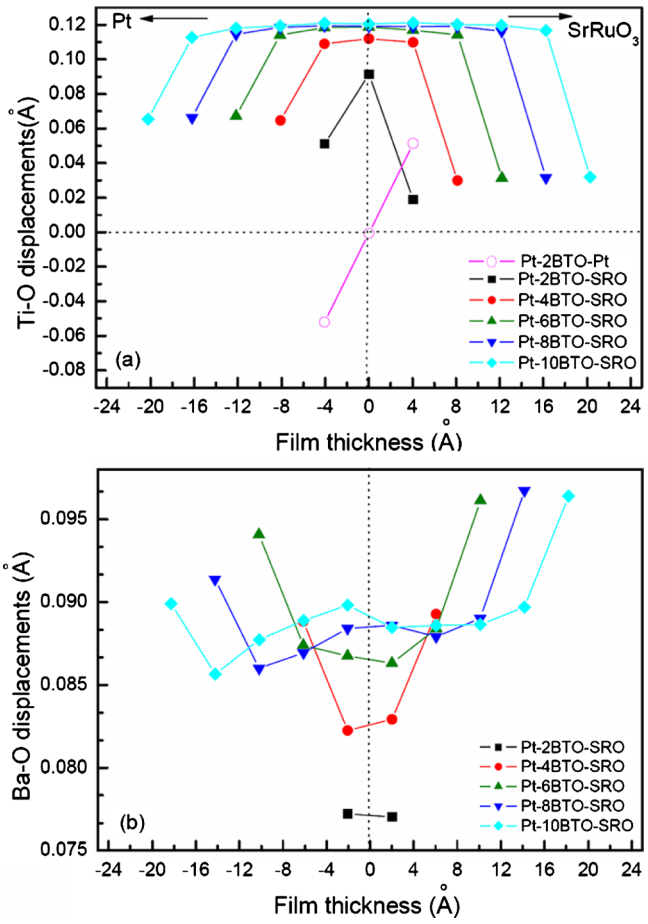

FIG. 2. (Color online) The relative Ti–O and Ba–O displacements along the bulk tetragonal soft mode *z*-axis direction with the fully relaxed configurations $[Pt_{10}/TiO_2-(BaO-TiO2)_n-(SrO-RuO_2)_3]$ (as shown in Fig. 1) as a function of the film thickness for different $n=2$, 4, 6, 8, and 10, respectively. In order to compare, the data of relative Ti–O displacements in a two layers ferroelectric $BaTiO_3$ film ($n=2$) with symmetric top and bottom Pt electrodes are also presented.

both figures, the RACDs at various depths in the films are plotted, for different film thicknesses. Here the zero-depth reference line is set at the midline of the film. A positive RACD gives an upward local electric dipole moment, and a negative one, vice versa (see Fig. 1). The corresponding Ti–O displacements in a two-unit cell (i.e., $n=2$) thick FTF in a S-FTJ with similar Pt electrodes are also presented in Fig. 2(a). Compared with the S-FTJ, the nonzero RACD in the A-FTJ clearly stands out.

Paraelectric $BaTiO_3$ can be recognized by an atomic configuration in which (1) the Ti and O ions are on the same plane, i.e., without *z*-direction relative displacements, (2) the situation is the same for the Ba and O ions, and (3) the in-plane net polarization is also zero.[11] In Fig. 2, it is clear that both the Ti–O and Ba–O displacements are positive, and the polarization is nonzero for all film thicknesses down to and including the 0.8 nm two-unit cell thick film (TCF). In contrast, the TCF in the S-FTJ is paraelectric, as shown in previous studies.[25] Indeed, all previous calculations found that $BaTiO_3$ capacitors or tunnel junctions, with symmetric Pt or $SrRuO_3$ electrodes under the short-circuit boundary conditions (zero bias), has critical thicknesses larger than 1.2 nm. This is true even for calculations where the GGA is

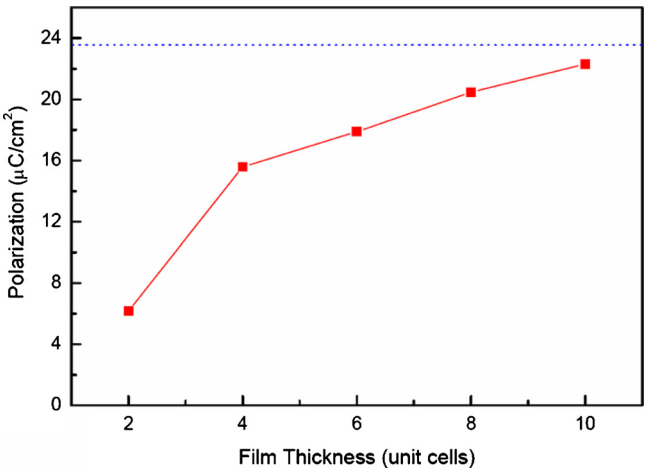

FIG. 3. (Color online) The polarization calculated as a function of FTF thickness (unit cells). The dotted line represents the calculated tetragonal bulk value.

adopted, which usually overestimates ferroelectric properties.[24,25] It is noteworthy that the Ti–O displacements in Fig. 2(a) have a smaller value at the ferroelectric-electrode interface, which quickly increases to the bulk value away from the interfacial region into the film. This shows that the penetration depths of the interface effect is limited to only one or two atomic distances, and supports the notion of surface-induced suppression of polarization suggested by experiments.[38]

B. The polarization as a function of FTF thickness

We calculate the total polarization P using the Berry phase method[34] by evaluating $P=\Sigma Z^* U$, where Z^* is the Born effective charge of each ion and U is the displacement of the ion from its position in the paraelectric stable state. Here the values of Z^* and U are obtained from the PWSCF package of the QUANTUM-ESPRESSO distribution.[39] Figure 3 shows the results of P (net dipole moment per unit volume) as a function of the $BaTiO_3$ film thickness (in terms of unit cells), here P only points to the electrode with higher work function (WF), i.e., Pt. P can be seen to increase gradually, approaching the bulk value (dotted line) with thicker films, as the interface that suppresses the polarization[38] moves farther away. The dotted line in Fig. 3 is calculated with a full relaxation taking into account the in-plane constraint due to the $SrTiO_3$ substrate, and represents the theoretic value of P for the tetragonal bulk. We note that as a result of the lattice relaxation, the dynamic charges near the interface are different from those in the bulk.

The foregoing results show that in the A-FTJ, ferroelectric $BaTiO_3$ films are stable in the monodomain configuration for thicknesses down to two unit cells or 0.8 nm (the minimum bulk size[40]). Although ferroelectricity has been found to exist in monolayer thin film of ferroelectric polymers,[12,13] the two-unit-cell thick $BaTiO_3$ film may be the thinnest of viable ferroelectric perovskite films. The findings in the foregoing bring us a big step closer to achieving the ultimate limit of the single-molecule ferroelectric memory element. In contrast, investigations show that the FTF in S-FTJs such as

the $SrRuO_3/KNbO_3/SrRuO_3$ capacitor, which is sufficiently thick to retain its ferroelectric character, cannot be stable in the monodomain form, but must contain the opposite domain near the interfaces with cancelling dipole moments.[23]

C. The macroscopic charge density and electrostatic potential in FTJ

Spontaneous polarization in a ferroelectric film creates bound charges of opposite signs near the opposite surfaces/interfaces of a ferroelectric capacitor, which produces a depolarization field with strength that increases quickly as the FTF gets thinner. The cancellation of the spontaneous polarization by the depolarization field is a main cause of the existence of a critical thickness, below which ferroelectricity disappears. It is well known that under short-circuit boundary conditions, charge transfer between the electrodes driven by the depolarization field leads to the screening of the depolarization charges and stabilize ferroelectricity of the film. Within the classical electrostatic treatment, the depolarization and screening charges are both assumed to lie on the ferroelectric-electrode interface, and the screening is 100% efficient, leading to the complete cancellation of the depolarization field. When the situation is considered quantum-mechanically in the atomic scale, taking into account the relaxation of the spontaneous polarization near the interfaces, the actual charge redistribution does not allow 100% screening of the depolarization charges. Besides the depolarization field, the charge transfer between the electrodes is also driven by the difference between their electronic environments that can be characterized in terms of parameters like the WFs or WF steps.[41,42]

In Fig. 4(a), we plot the macroscopically averaged charge densities,[14] i.e., ionic plus electronic, at different locations of the A-FTJ. Bound charges in the FTF near the two ferroelectric-electrode interfaces produce the unscreened depolarization field E_{ud}. In response to this field the mobile charges redistribute inside and between the electrodes self-consistently. The redistribution is driven by energy minimization according to two main factors, (1) the presence of the screening charges in the two electrodes, which induce the charge screening electric field E_{cs} (Ref. 14) and (2) the difference between the electronic environments such as Fermi levels (FLs) in the two electrodes, which induce the build-in electric field E_i. The total electric field in A-FTJ defines the critical thickness consists of the unscreened depolarization field E_{ud} counteracted by the electric field produced by the charge redistribution driven by the combined actions of the two factors. In this regard, the charge redistribution in response to the depolarization charges leads to the charge screening field E_{cs},[14] and that driven by the Fermi energy difference creates a build-in electric field E_i. The electrostatic potential corresponding to the total electric field is plotted in Fig. 4(b) (black line). The practically flat potential indicates the near complete cancellation of E_{ud} by $E_{cs}+E_i$ that arises from the charge redistribution in the electrodes, which explains the absence of critical thickness obtained in our calculation. This can also be considered more quantitatively from another angle.

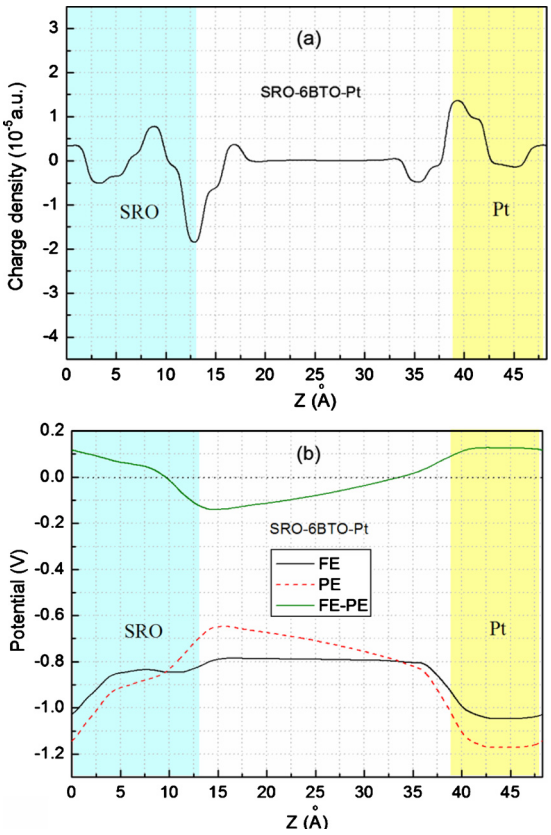

FIG. 4. (Color online) (a) The macroscopic total (ionic plus electronic) charge density. (b) The macroscopic-averaged electrostatic potential [black line (bottom)], which include the contribution of the unscreened depolarizing field E_{ud}, charge screening electric field E_{cs} and built-in electric field E_i (as shown in Fig. 1), for the fully relaxed $BaTiO_3$ (BTO) FTJ is shown. In order to show the existence of the built-in electric field E_i caused by the dissimilar electrodes Pt and $SrRuO_3$ (SRO) with the different electronic environment of the two electrodes in the short-circuited conditions, the electrostatic potential of $BaTiO_3$ film (red dashed line) with the original paraelectric configurations is also presented. Moreover, the green line (top) represents the difference of electrostatic potential between the paraelectric (PE) and ferroelectric (FE) phases.

While charge transfer between the two electrodes driven to screen E_{ud} under short-circuit boundary conditions is a well-known phenomenon, which driven by the asymmetry of the electrodes is less apparent.[16] To understand the role of the latter, we calculate the electrostatic potential across a short-circuited A-FTJ with a $BaTiO_3$ film in paraelectric phase, i.e., without the polarization and depolarization fields, and present it as the red dash line in Fig. 4(b). Without depolarization and screening, the corresponding electric field is E_i created by the charge transfer between the dissimilar electrodes is only due to their different electronic environments.[16,41] From the slope of the red dash line in Fig. 4(b), the magnitude of E_i in the paraelectric $BaTiO_3$ film can be calculated and is found to be very significant, $\sim -0.70 \times 10^8$ (V/m). At the same time, if one may use this value to estimate E_i in the ferroelectric $BaTiO_3$ film, then noting that the total electric field is a sum of the fields E_{ud}, E_{cs}, and E_i, the field from the screened depolarization charges $E_{ud}+E_{cs}$ may be estimated from the difference between the black and red dash curves, which is plotted as the green line in Fig. 4(b). From the slope of the green line the value of $E_{ud}+E_{cs}$

can be estimated to be $\sim 0.763 \times 10^8$ (V/m), which is almost completely canceled by the field E_i created by the asymmetry of the electrodes. In this regard, we note that in the case of S-FTJ with the symmetric electrodes, E_i would vanish and the final depolarization field $E_d = E_{ud} + E_{cs}$, which is a well-defined and well-established result.[7,16,17] In this case, the value of the total electric field in S-FTJ is only determined by the depolarization field, which can result in the presence of a critical thickness.

Indeed, the existence of a large built-in electric field in a thin insulating film sandwiched between electrodes with different FL or WFs under short-circuited conditions has been suggested previously.[41] This electric field increases with decreasing film thickness as the interfaces move closer together and becomes very strong in ultrathin films. The strength of the built-in electric field may be estimated by $E_i = (W_2 - W_1)/ed$ (Ref. 41) or $E_i = -(\Delta\varphi_2 - \Delta\varphi_1)/d$,[42] where W_1, W_2 and $\Delta\varphi_1$, $\Delta\varphi_2$ are the WFs of electrodes and WF steps across the $BaTiO_3$/Pt and $BaTiO_3$/$SrRuO_3$ interfaces, respectively, and d is the thickness of the barrier layer. Based on WFs of 5.65 eV and 5.2 eV for Pt and $SrRuO_3$,[43,44] respectively, one may estimate $E_i \approx 1.875 \times 10^8$ (V/m) for a $BaTiO_3$ barrier with thickness of 2.4 nm ($n=6$), which is higher than that obtained from the present calculations ($\sim 0.70 \times 10^8$ V/m). The main reason for this difference is the relaxation of the lattice configuration near the ferroelectric/electrode region, which is fully accounted for in our simulations, unlike the thermodynamic estimations. For the same reasons, it can also be seen that the unscreened depolarization field E_{ud} we obtained ($\sim 0.763 \times 10^8$ V/m) is much smaller than that predicted by the thermodynamic theory by Pertsev and Kohlstedt[26] (i.e., $\sim 1.2 \times 10^8$ V/m) or Zheng and Woo[7] (i.e., $\sim 1.4 \times 10^8$ V/m) for the A-FTJ at 0 K.

The existence of a built-in electric field trims down the effects of the depolarization field in ultrathin ferroelectric films and allows the spontaneous polarization to persist as the film thickness diminishes, thus drastically reducing the critical thickness in the cases studied. In this way, via the use of dissimilar electrodes, adverse effects of the depolarization field on the critical thickness may be controlled and adjusted in actual applications of FTJs. For example, an asymmetric system, i.e., tip electrode/FTF/semiconductor substrate (TE/FTF/SS), was recently studied within the framework of Landau–Ginzburg–Devonshire phenomenology by Morozovska *et al.*[45] They also obtained that a built-in field support the polarization in the ferroelectric film under the absence of applied electric field. At the same time, Morozovska *et al.*[45] applied the external electric field to the asymmetric heterostructure and studied the hysteresis loop shape of TE/FTF/SS structure, their results shown that despite pronounced nonzero polarization exists in the ultrathin ferroelectric film, hysteresis loops disappears at thicknesses $L < L_{cr}$, and indicated that some critical thickness defined with respect to the hysteresis loop may disappear. These interesting results should be investigated and discussed using the first principle calculations in future. Moreover, the multi-FTJs (M-FTJs) with ferroelectric or multiferroic barriers sandwiched between two magnetic electrodes also attract broad interest.[46–51] It is highly desirable to explore the interaction between dissimilar electrodes and critical size for A-FTJs and A-MFTJs in future experimental and theoretical studies.

IV. CONCLUSIONS

In summary, we performed first-principle density-functional calculations of the electronic states and equilibrium ionic configurations in an A-FTJ, i.e., one with dissimilar electrodes, from which the charge distributions and polarization were obtained. In contrast to symmetric FTJs (S-FTJ), for which ferroelectricity disappear below a critical thickness. The polarization pointing to the electrode with higher WF, i.e., Pt, was found to be significant and stable in a $BaTiO_3$ superthin film between Pt and $SrRuO_3$ electrodes, with film thicknesses even down to 0.8 nm (two unit-cells). This surprising result was traced to the cancellation of the depolarization field by the large electric field generated by the charge transfer between the electrodes which arose due to the different electronic environments. We speculate that this is a general result for A-FTJs, which could have significant impact on the functional design of FTJs or capacitors in next-generation nanoscaled ferroelectric devices where the presence of the critical thickness is a serious challenge to efforts of further miniaturization. We note that our present findings are obtained through a theoretical analysis. Confirmation by further investigations, experimental, in particular, is needed.

ACKNOWLEDGMENTS

This work was initiated and performed under leadership of C. H. Woo and Y. Zheng of Department of Electronic and Information Engineering of HK PolyU, to whom correspondence and requests for materials should be directed. Funding support for this work is from the RGC of the HK SAR (Grant Nos. G-YX0T, 5322/04E, and N53408). Y. Zheng and M. Q. Cai are also grateful for support from the NSFC (Grant Nos. 50802026 and 10902128) and Creative Research Group of NSFC (Grant No. 50721003). Helpful discussions with E. Y. Tsymbal, J. P. Velev, J. Junquera, P. Ghosez, A. K. Tagantsev, and C. G. Duan are also gratefully acknowledged.

[1] V. Garcia, S. Fusil, K. Bouzehouane, S. E. Vedrenne, N. D. Mathur, A. Barthelemy, and M. Bibes, Nature (London) **460**, 81 (2009).
[2] P. Maksymovych, S. Jesse, P. Yu, R. Ramesh, A. P. Baddorf, and S. V. Kalinin, Science **324**, 1421 (2009).
[3] M. Y. Zhuravlev, R. F. Sabirianov, S. S. Jaswal, and E. Y. Tsymbal, Phys. Rev. Lett. **94**, 246802 (2005).
[4] R. Waser and M. Aono, Nature Mater. **6**, 833 (2007).
[5] E. Y. Tsymbal and H. Kohlstedt, Science **313**, 181 (2006).
[6] A. Gruverman, D. Wu, H. Lu, Y. Wang, H. W. Jang, C. M. Folkman, M. Y. Zhuravlev, D. Felker, M. Rzchowski, C. B. Eom, and E. Y. Tsymbal, Nano Lett. **9**, 3539 (2009).
[7] Y. Zheng and C. H. Woo, Nanotechnology **20**, 075401 (2009).
[8] T. Tybell, C. H. Ahn, and J. M. Triscone, Appl. Phys. Lett. **75**, 856 (1999).
[9] D. D. Fong, G. B. Stephenson, S. K. Streiffer, J. A. Eastman, O. Auciello, P. H. Fuoss, and C. Thompson, Science **304**, 1650 (2004).
[10] D. D. Fong, A. M. Kolpak, J. A. Eastman, S. K. Streiffer, P. H. Fuoss, G. B. Stephenson, C. Thompson, D. M. Kim, K. J. Choi, C. B. Eom, I. Grinberg, and A. M. Rappe, Phys. Rev. Lett. **96**, 127601 (2006).
[11] D. A. Tenne, P. Turner, J. D. Schmidt, M. Biegalski, Y. L. Li, L. Q. Chen, A. Soukiassian, S. Trolier-McKinstry, D. G. Schlom, X. X. Xi, D. D. Fong, P. H. Fuoss, J. A. Eastman, G. B. Stephenson, C. Thompson, and S. K. Streiffer, Phys. Rev. Lett. **103**, 177601 (2009).
[12] A. V. Bune, V. M. Fridkin, S. Ducharme, L. M. Blinov, S. P. Palto, A. V.

Sorokin, S. G. Yudin, and A. Zlatkin, Nature (London) **391**, 874 (1998).
[13]Z. J. Hu, M. W. Tian, B. Nysten, and A. M. Jonas, Nature Mater. **8**, 62 (2009).
[14]J. Junquera and P. Ghosez, Nature (London) **422**, 506 (2003).
[15]B. Wang and C. H. Woo, J. Appl. Phys. **97**, 084109 (2005).
[16]Y. Zheng, M. Q. Cai, and C. H. Woo, Acta Mater. **58**, 3050 (2010).
[17]Y. Zheng, C. H. Woo, and B. Wang, Nano Lett. **8**, 3131 (2008).
[18]M. Q. Cai, Y. Zheng, B. Wang, and G. W. Yang, Appl. Phys. Lett. **95**, 232901 (2009).
[19]M. E. Lines and A. M. Glass, *Principles and Applications of Ferroelectrics and Related Materials* (Clarendon, Oxford, 1977).
[20]M. Stengel, D. Vanderbilt, and N. A. Spaldin, Nature Mater. **8**, 392 (2009).
[21]A. M. Kolpak, I. Grinberg, and A. M. Rappe, Phys. Rev. Lett. **98**, 166101 (2007).
[22]M. Nuñez and M. B. Nardelli, Phys. Rev. Lett. **101**, 107603 (2008).
[23]C. G. Duan, R. F. Sabirianov, W. N. Mei, S. S. Jaswai, and E. Y. Tsymbal, Nano Lett. **6**, 483 (2006).
[24]Y. Umeno, B. Meyer, C. Elsasser, and P. Gumbsch, Phys. Rev. B **74**, 060101 (2006).
[25]N. Sai, A. M. Kolpak, and A. M. Rappe, Phys. Rev. B **72**, 020101 (2005).
[26]N. A. Pertsev and H. Kohlstedt, Phys. Rev. Lett. **98**, 257603 (2007).
[27]X. Y. Wang, Y. L. Wang, and R. J. Yang, Appl. Phys. Lett. **95**, 142910 (2009).
[28]I. Ponomareva and L. Bellaiche, Phys. Rev. Lett. **101**, 197602 (2008).
[29]K. M. Rabe, Nat. Nanotechnol. **1**, 171 (2006).
[30]M. Stengel and N. A. Spaldin, Nature (London) **443**, 679 (2006).
[31]D. Vanderbilt, Phys. Rev. B **41**, 7892 (1990).
[32]D. M. Ceperley and B. J. Alder, Phys. Rev. Lett. **45**, 566 (1980).
[33]D. I. Bilc, R. Orlando, R. Shaltaf, G. M. Rignanese, J. Iniguez, and P. Ghosez, Phys. Rev. B **77**, 165107 (2008).
[34]R. D. King-Smith and D. Vanderbilt, Phys. Rev. B **47**, 1651 (1993).
[35]A. M. Kolpak, N. Sai, and A. M. Pappe, Phys. Rev. B **74**, 054112 (2006).
[36]R. E. Cohen, Nature (London) **358**, 136 (1992).
[37]G. Gerra, A. K. Tagantsev, and N. Setter, Phys. Rev. Lett. **98**, 207601 (2007).
[38]C. L. Jia, V. Nagarajan, J. Q. He, L. Houben, T. Zhao, R. Ramesh, K. Urban, and R. Waser, Nature Mater. **6**, 64 (2007).
[39]P. Giannozzi, S. Baroni, N. Bonini, M. Calandra, R. Car, C. Cavazzoni, D. Ceresoli, G. L. Chiarotti, M. Cococcioni, I. Dabo, A. Dal Corso, S. de Gironcolik, S. Fabris, G. Fratesi, R. Gebauer, U. Gerstmann, C. gougoussis, A. Kokalj, M. Lazzeri, L. Martin-Samos, N. Marzari, F. Mauri, R. Mazzarello, S. Paolini, A. Pasquarello, L. Paulatto, C. Sbraccia, S. Scandolo, G. Sclauzero, A. P. Seitsonen, A. Smogunov, P. Umari, and R. M. Wentzcovitch, J. Phys.: Condens. Matter **21**, 395502 (2009).
[40]N. Sai, C. J. Fennie, and A. A. Demkov, Phys. Rev. Lett. **102**, 107601 (2009).
[41]J. G. Simmons, Phys. Rev. Lett. **10**, 10 (1963).
[42]A. K. Tagantsev, G. Gerra, and N. Setter, Phys. Rev. B **77**, 174111 (2008).
[43]C. Yoshida, A. Yoshida, and H. Tamura, Appl. Phys. Lett. **75**, 1449 (1999).
[44]H. B. Michaelson, IBM J. Res. Dev. **22**, 72 (1978).
[45]A. N. Morozovska, E. A. Eliseev, S. V. Svechnikov, A. D. Krutov, V. Y. Shur, A. Y. Borisevich, P. Maksymovych, and S. V. Kalinin, Phys. Rev. B **81**, 205308 (2010).
[46]J. P. Velev, C. G. Duan, J. D. Burton, A. Smogunov, M. K. Niranjan, E. Tosatti, S. S. Jaswai, and E. Y. Tsymbal, Nano Lett. **9**, 427 (2009).
[47]J. Seidel, L. W. Martin, Q. He, Q. Zhan, Y. H. Chu, A. Rother, M. E. Hawkridge, P. Maksymovych, P. Yu, M. Gajek, N. Balke, S. V. Kalinin, S. Gemming, F. Wang, G. Catalan, J. F. Scott, N. A. Spaldin, J. Orenstein, and R. Ramesh, Nature Mater. **8**, 229 (2009).
[48]H. Zheng, J. Wang, S. E. Lofland, Z. Ma, L. Mohaddes-Ardabili, T. Zhao, L. Salamanca-Riba, S. R. Shinde, S. B. Ogale, F. Bai, D. Viehland, Y. Jia, D. G. Schlom, M. Wuttig, A. Roytburd, and R. Ramesh, Science **303**, 661 (2004).
[49]M. Gajek, M. Bibes, S. Fusil, K. Bouzehouane, J. Fontcuberta, A. E. Barthelemy, and A. Fert, Nature Mater. **6**, 296 (2007).
[50]Y. Tokunaga, N. Furukawa, H. Sakai, Y. Taguchi, T. H. Arima, and Y. Tokura, Nature Mater. **8**, 558 (2009).
[51]S. W. Cheong and M. Mostovoy, Nature Mater. **6**, 13 (2007).